

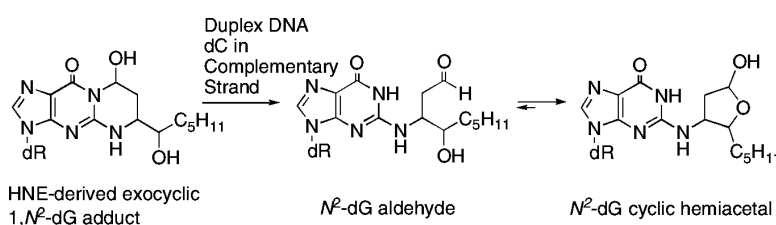
Article

Rearrangement of the (6*S*,8*R*,11*S*) and (6*R*,8*S*,11*R*) Exocyclic 1,*N*-Deoxyguanosine Adducts of *trans*-4-Hydroxynonenal to *N*-Deoxyguanosine Cyclic Hemiacetal Adducts When Placed Complementary to Cytosine in Duplex DNA

Hai Huang, Hao Wang, Nan Qi, Albena Kozekova, Carmelo J. Rizzo, and Michael P. Stone

J. Am. Chem. Soc., **2008**, 130 (33), 10898-10906 • DOI: 10.1021/ja801824b • Publication Date (Web): 29 July 2008

Downloaded from <http://pubs.acs.org> on February 8, 2009



More About This Article

Additional resources and features associated with this article are available within the HTML version:

- Supporting Information
- Links to the 2 articles that cite this article, as of the time of this article download
- Access to high resolution figures
- Links to articles and content related to this article
- Copyright permission to reproduce figures and/or text from this article

[View the Full Text HTML](#)

Rearrangement of the (6*S*,8*R*,11*S*) and (6*R*,8*S*,11*R*) Exocyclic 1,*N*²-Deoxyguanosine Adducts of *trans*-4-Hydroxynonenal to *N*²-Deoxyguanosine Cyclic Hemiacetal Adducts When Placed Complementary to Cytosine in Duplex DNA

Hai Huang, Hao Wang, Nan Qi, Albena Kozekova, Carmelo J. Rizzo, and Michael P. Stone*

Department of Chemistry and Center in Molecular Toxicology, Vanderbilt University, Nashville, Tennessee 37235

Received March 11, 2008; E-mail: michael.p.stone@vanderbilt.edu

Abstract: *trans*-4-Hydroxynonenal (HNE) is a peroxidation product of ω -6 polyunsaturated fatty acids. The Michael addition of deoxyguanosine to HNE yields four diastereomeric exocyclic 1,*N*²-dG adducts. The corresponding acrolein- and crotonaldehyde-derived exocyclic 1,*N*²-dG adducts undergo ring-opening to *N*²-dG aldehydes, placing the aldehyde functionalities into the minor groove of DNA. The acrolein- and the 6*R*-crotonaldehyde-derived exocyclic 1,*N*²-dG adducts form interstrand *N*²-dG:*N*²-dG cross-links in the 5'-CpG-3' sequence context. Only the HNE-derived exocyclic 1,*N*²-dG adduct of (6*S*,8*R*,11*S*) stereochemistry forms interstrand *N*²-dG:*N*²-dG cross-links in the 5'-CpG-3' sequence context. Moreover, as compared to the exocyclic 1,*N*²-dG adducts of acrolein and crotonaldehyde, the cross-linking reaction is slow (Wang, H.; Kozekov, I. D.; Harris, T. M.; Rizzo, C. J. *J. Am. Chem. Soc.* **2003**, *125*, 5687–5700). Accordingly, the chemistry of the HNE-derived exocyclic 1,*N*²-dG adduct of (6*S*,8*R*,11*S*) stereochemistry has been compared with that of the (6*R*,8*S*,11*R*) adduct, when incorporated into 5'-d(GCTAGCXAGTCC)-3'·5'-d(G-GACTCGCTAGC)-3', containing the 5'-CpG-3' sequence (X = HNE-dG). When placed complementary to dC in this duplex, both adducts open to the corresponding *N*²-dG aldehydic rearrangement products, suggesting that the formation of the interstrand cross-link by the exocyclic 1,*N*²-dG adduct of (6*S*,8*R*,11*S*) stereochemistry, and the lack of cross-link formation by the exocyclic 1,*N*²-dG adduct of (6*R*,8*S*,11*R*) stereochemistry, is not attributable to inability to undergo ring-opening to the aldehydes in duplex DNA. Instead, these aldehydic rearrangement products exist in equilibrium with stereoisomeric cyclic hemiacetals. The latter are the predominant species present at equilibrium. The *trans* configuration of the HNE H6 and H8 protons is preferred. The presence of these cyclic hemiacetals in duplex DNA is significant as they mask the aldehyde species necessary for interstrand cross-link formation.

Introduction

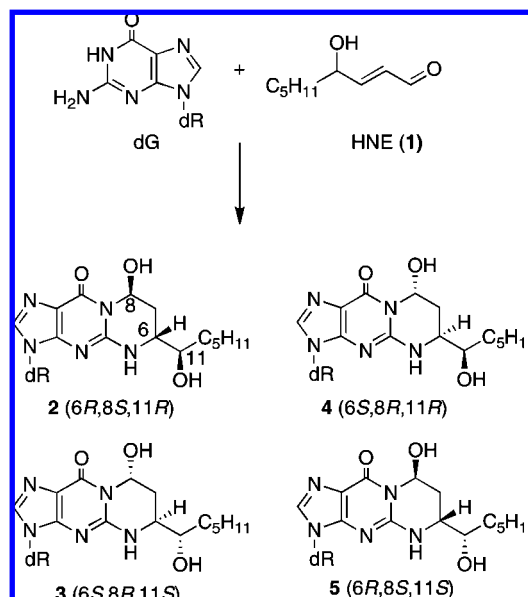
trans-4-Hydroxynonenal (**1**, HNE) is produced from the metabolism of membrane lipids,¹ and it is the major in vivo peroxidation product of ω -6 polyunsaturated fatty acids.^{2,3} Several routes for the formation of HNE from ω -6 polyunsaturated fatty acids have been described.^{4–6} HNE exhibits a range of biological effects, from alteration in gene expression and cell signaling to cell proliferation and apoptosis.^{7–13} Human exposure

to HNE has been implicated in the etiologies of a number of diseases associated with oxidative stress, including Alzheimer's disease,¹⁴ Parkinson's disease,¹⁵ arteriosclerosis,¹⁶ and hepatic ischemia reperfusion injury.¹⁷

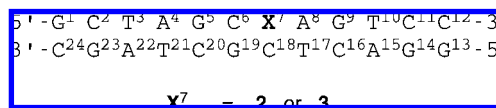
With regard to genotoxicity, HNE induces an SOS response in *Escherichia coli*.¹⁸ Chromosomal aberrations are observed

- (1) Benedetti, A.; Comporti, M.; Esterbauer, H. *Biochim. Biophys. Acta* **1980**, *620*, 281–296.
- (2) Esterbauer, H.; Schaur, R. J.; Zollner, H. *Free Radical Biol. Med.* **1991**, *11*, 81–128.
- (3) Burcham, P. C. *Mutagenesis* **1998**, *13*, 287–305.
- (4) Lee, S. H.; Blair, I. A. *Chem. Res. Toxicol.* **2000**, *13*, 698–702.
- (5) Schneider, C.; Tallman, K. A.; Porter, N. A.; Brash, A. R. *J. Biol. Chem.* **2001**, *276*, 20831–20838.
- (6) Schneider, C.; Porter, N. A.; Brash, A. R. *J. Biol. Chem.* **2008**, *283*, 15539–15543.
- (7) Parola, M.; Bellomo, G.; Robino, G.; Barrera, G.; Dianzani, M. U. *Antioxid. Redox Signaling* **1999**, *1*, 255–284.
- (8) Poli, G.; Schaur, R. J. *IUBMB Life* **2000**, *50*, 315–321.
- (9) Nakashima, I.; Liu, W.; Akhand, A. A.; Takeda, K.; Kawamoto, Y.; Kato, M.; Suzuki, H. *Mol. Aspects Med.* **2003**, *24*, 231–238.

- (10) West, J. D.; Ji, C.; Duncan, S. T.; Amarnath, V.; Schneider, C.; Rizzo, C. J.; Brash, A. R.; Marnett, L. J. *Chem. Res. Toxicol.* **2004**, *17*, 453–462.
- (11) West, J. D.; Marnett, L. J. *Chem. Res. Toxicol.* **2005**, *18*, 1642–1653.
- (12) West, J. D.; Marnett, L. J. *Chem. Res. Toxicol.* **2006**, *19*, 173–194.
- (13) Dwivedi, S.; Sharma, A.; Patrick, B.; Sharma, R.; Awasthi, Y. C. *Redox Rep.* **2007**, *12*, 4–10.
- (14) Sayre, L. M.; Zelasko, D. A.; Harris, P. L.; Perry, G.; Salomon, R. G.; Smith, M. A. *J. Neurochem.* **1997**, *68*, 2092–2097.
- (15) Yoritaka, A.; Hattori, N.; Uchida, K.; Tanaka, M.; Stadtman, E. R.; Mizuno, Y. *Proc. Natl. Acad. Sci. U.S.A.* **1996**, *93*, 2696–2701.
- (16) Napoli, C.; D'Armiento, F. P.; Mancini, F. P.; Postiglione, A.; Witztum, J. L.; Palumbo, G.; Palinski, W. *J. Clin. Invest.* **1997**, *100*, 2680–2690.
- (17) Yamagami, K.; Yamamoto, Y.; Kume, M.; Ishikawa, Y.; Yamaoka, Y.; Hiai, H.; Toyokuni, S. *Antioxid. Redox Signaling* **2000**, *2*, 127–136.
- (18) Benamira, M.; Marnett, L. J. *Mutat. Res.* **1992**, *293*, 1–10.

Chart 1. Formation of Exocyclic 1,N²-dG Adducts 2-5 by HNE

upon exposure to HNE in rodent,^{19,20} mammalian,^{21,22} and human²³ cells. In mammalian cells, the genotoxicity of HNE depends upon glutathione levels, which modulate the formation of HNE-DNA adducts.^{24–26} Michael addition of the N²-amino group of deoxyguanosine to HNE gives four diastereomeric exocyclic 1,N²-dG adducts 2–5 (Chart 1),^{27–29} which have been detected in cellular DNAs.^{30–36} Alternatively, oxidation of HNE to 2,3-epoxy-4-hydroxynonanal, and further reaction with nucleobases, affords substituted etheno adducts.^{37–41}

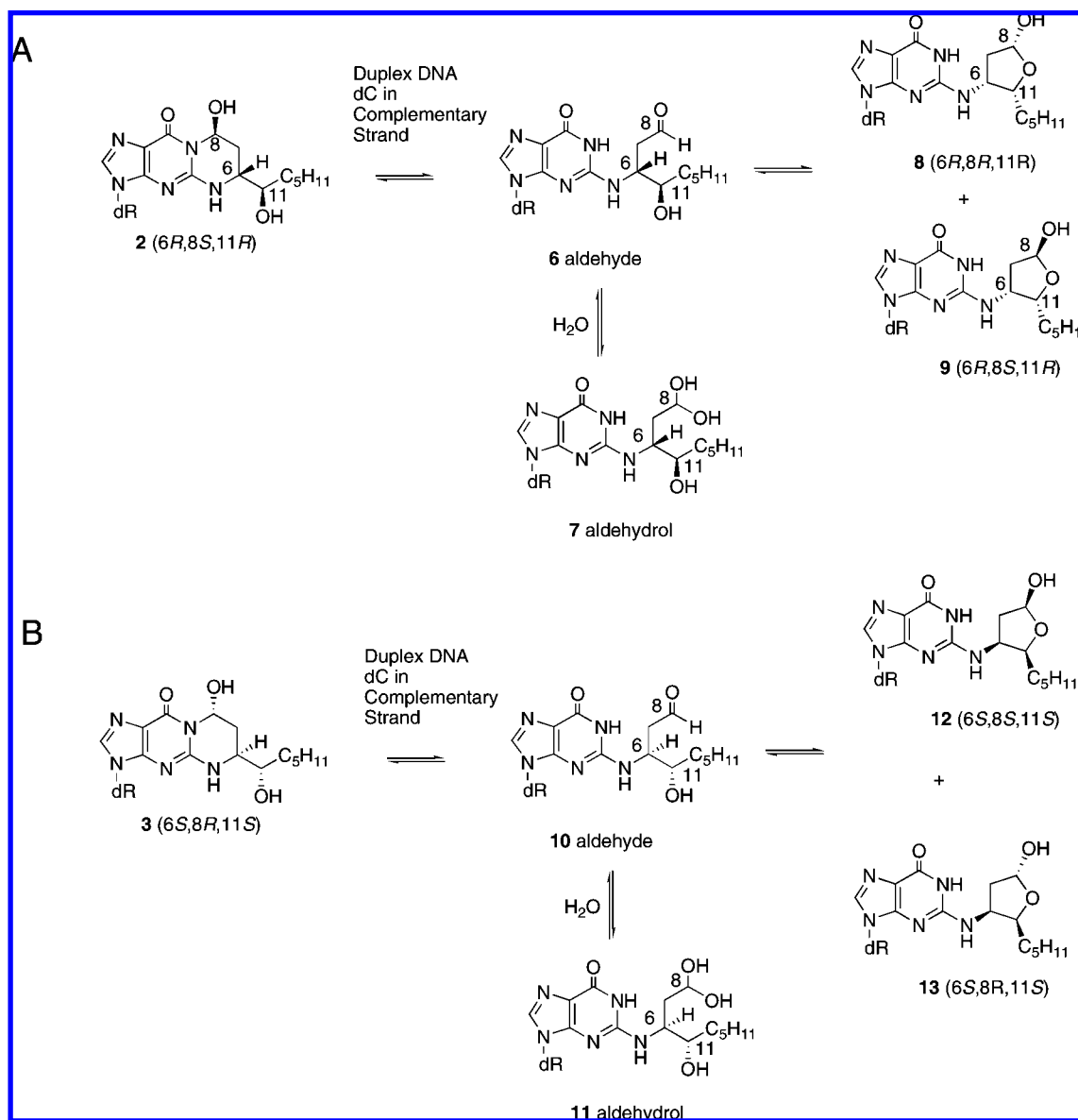
Chart 2. Nucleotide Numbering Scheme of the Dodecamer Containing the 5'-C⁶pX⁷-3' Sequence Context; X Represents the Position of the HNE-Derived Exocyclic 1,N²-dG Adducts 2 or 3

The mutational spectrum induced by HNE in the *lacZ* gene of the single-stranded M13 phage transfected into wild-type *E. coli* revealed recombination events, C → T transitions, followed by G → C and A → C transversions, and frameshift mutations.²⁹ HNE is mutagenic⁴² and carcinogenic in rodent cells.⁴³ Hussain et al.⁴⁴ reported that HNE caused G•C → T•A transversions at codon 249 of wild-type *p53* in lymphoblastoid cells. Hu et al.⁴⁵ further reported that HNE-DNA adducts were preferentially formed with guanine at the third base of codon 249 in the *p53* gene. The mutational spectrum induced by *trans*-4-hydroxynonanal-derived deoxyguanosine (HNE-dG) adducts in the *supF* gene of shuttle vector pSP189 replicated in human cells showed that HNE induced primarily G → T transversions, accompanied by lower levels of G → A transitions.⁴⁶ Fernandes et al.⁴⁷ conducted site-specific mutagenesis studies and observed that, in the 5'-CpG-3' duplex of interest in the present work, only stereoisomers 2 and 3 of the HNE-induced exocyclic 1,N²-dG adduct were mutagenic, inducing low levels of G → T transversions and G → A transitions. Evidence has been obtained that nucleotide excision repair pathway is involved in the repair of HNE-dG lesion.^{46,48,49}

Wang et al.^{50,51} synthesized the four stereoisomers of the HNE-derived exocyclic 1,N²-dG Michael addition products (2–5) and incorporated them into 5'-d(GCTAGCXAGTCC)-3'•5'-d(GGACTCGCTAGC)-3', in which X denotes the HNE-dG adduct (Chart 2). The related deoxyguanosine adducts of acrolein^{52–55} and crotonaldehyde⁵⁶ formed interchain cross-links

- (19) Esterbauer, H.; Eckl, P.; Ortner, A. *Mutat. Res.* **1990**, *238*, 223–233.
 (20) Eckl, P. M.; Ortner, A.; Esterbauer, H. *Mutat. Res.* **1993**, *290*, 183–192.
 (21) Karlhuber, G. M.; Bauer, H. C.; Eckl, P. M. *Mutat. Res.* **1997**, *381*, 209–216.
 (22) Eckl, P. M. *Mol. Aspects Med.* **2003**, *24*, 161–165.
 (23) Emerit, I.; Khan, S. H.; Esterbauer, H. *Free Radical Biol. Med.* **1991**, *10*, 371–377.
 (24) Chung, F. L.; Komninou, D.; Zhang, L.; Nath, R.; Pan, J.; Amin, S.; Richie, J. *Chem. Res. Toxicol.* **2005**, *18*, 24–27.
 (25) Falletti, O.; Cadet, J.; Favier, A.; Douki, T. *Free Radical Biol. Med.* **2007**, *42*, 1258–1269.
 (26) Yadav, U. C.; Ramana, K. V.; Awasthi, Y. C.; Srivastava, S. K. *Toxicol. Appl. Pharmacol.* **2008**, *227*, 257–264.
 (27) Winter, C. K.; Segall, H. J.; Haddon, W. F. *Cancer Res.* **1986**, *46*, 5682–5686.
 (28) Douki, T.; Odin, F.; Caillat, S.; Favier, A.; Cadet, J. *Free Radical Biol. Med.* **2004**, *37*, 62–70.
 (29) Kowalczyk, P.; Ciesla, J. M.; Komisarowski, M.; Kusmirek, J. T.; Tudek, B. *Mutat. Res.* **2004**, *550*, 33–48.
 (30) Yi, P.; Zhan, D.; Samokyszyn, V. M.; Doerge, D. R.; Fu, P. P. *Chem. Res. Toxicol.* **1997**, *10*, 1259–1265.
 (31) Chung, F. L.; Nath, R. G.; Ocando, J.; Nishikawa, A.; Zhang, L. *Cancer Res.* **2000**, *60*, 1507–1511.
 (32) Wacker, M.; Schuler, D.; Wanek, P.; Eder, E. *Chem. Res. Toxicol.* **2000**, *13*, 1165–1173.
 (33) Wacker, M.; Wanek, P.; Eder, E. *Chem.-Biol. Interact.* **2001**, *137*, 269–283.
 (34) Chung, F. L.; Zhang, L. *Methods Enzymol.* **2002**, *353*, 523–536.
 (35) Liu, X.; Lovell, M. A.; Lynn, B. C. *Chem. Res. Toxicol.* **2006**, *19*, 710–718.
 (36) Pan, J.; Davis, W.; Trushin, N.; Amin, S.; Nath, R. G.; Salem, N., Jr.; Chung, F. L. *Anal. Biochem.* **2006**, *348*, 15–23.
 (37) Sodum, R. S.; Chung, F. L. *Cancer Res.* **1988**, *48*, 320–323.
 (38) Sodum, R. S.; Chung, F. L. *Chem. Res. Toxicol.* **1989**, *2*, 23–28.
 (39) Sodum, R. S.; Chung, F. L. *Cancer Res.* **1991**, *51*, 137–143.
 (40) Chen, H. J.; Chung, F. L. *Chem. Res. Toxicol.* **1994**, *7*, 857–860.
 (41) el Ghissassi, F.; Barbin, A.; Nair, J.; Bartsch, H. *Chem. Res. Toxicol.* **1995**, *8*, 278–283.

- (42) Cajelli, E.; Ferraris, A.; Brambilla, G. *Mutat. Res.* **1987**, *190*, 169–171.
 (43) Chung, F. L.; Chen, H. J.; Guttenplan, J. B.; Nishikawa, A.; Hard, G. C. *Carcinogenesis* **1993**, *14*, 2073–2077.
 (44) Hussain, S. P.; Raja, K.; Amstad, P. A.; Sawyer, M.; Trudel, L. J.; Wogan, G. N.; Hofseth, L. J.; Shields, P. G.; Billiar, T. R.; Trautwein, C.; Hohler, T.; Galle, P. R.; Phillips, D. H.; Markin, R.; Marrogi, A. J.; Harris, C. C. *Proc. Natl. Acad. Sci. U.S.A.* **2000**, *97*, 12770–12775.
 (45) Hu, W.; Feng, Z.; Eveleigh, J.; Iyer, G.; Pan, J.; Amin, S.; Chung, F. L.; Tang, M. S. *Carcinogenesis* **2002**, *23*, 1781–1789.
 (46) Feng, Z.; Hu, W.; Amin, S.; Tang, M. S. *Biochemistry* **2003**, *42*, 7848–7854.
 (47) Fernandes, P. H.; Wang, H.; Rizzo, C. J.; Lloyd, R. S. *Environ. Mol. Mutagen.* **2003**, *42*, 68–74.
 (48) Chung, F. L.; Pan, J.; Choudhury, S.; Roy, R.; Hu, W.; Tang, M. S. *Mutat. Res.* **2003**, *531*, 25–36.
 (49) Choudhury, S.; Pan, J.; Amin, S.; Chung, F. L.; Roy, R. *Biochemistry* **2004**, *43*, 7514–7521.
 (50) Wang, H.; Rizzo, C. J. *Org. Lett.* **2001**, *3*, 3603–3605.
 (51) Wang, H.; Kozekov, I. D.; Harris, T. M.; Rizzo, C. J. *J. Am. Chem. Soc.* **2003**, *125*, 5687–5700.
 (52) Kozekov, I. D.; Nechev, L. V.; Sanchez, A.; Harris, C. M.; Lloyd, R. S.; Harris, T. M. *Chem. Res. Toxicol.* **2001**, *14*, 1482–1485.
 (53) Kozekov, I. D.; Nechev, L. V.; Moseley, M. S.; Harris, C. M.; Rizzo, C. J.; Stone, M. P.; Harris, T. M. *J. Am. Chem. Soc.* **2003**, *125*, 50–61.
 (54) Kim, H. Y.; Voehler, M.; Harris, T. M.; Stone, M. P. *J. Am. Chem. Soc.* **2002**, *124*, 9324–9325.
 (55) Cho, Y. J.; Kim, H. Y.; Huang, H.; Slutsky, A.; Minko, I. G.; Wang, H.; Nechev, L. V.; Kozekov, I. D.; Kozekova, A.; Tamura, P.; Jacob, J.; Voehler, M.; Harris, T. M.; Lloyd, R. S.; Rizzo, C. J.; Stone, M. P. *J. Am. Chem. Soc.* **2005**, *127*, 17686–17696.
 (56) Cho, Y. J.; Wang, H.; Kozekov, I. D.; Kurtz, A. J.; Jacob, J.; Voehler, M.; Smith, J.; Harris, T. M.; Lloyd, R. S.; Rizzo, C. J.; Stone, M. P. *Chem. Res. Toxicol.* **2006**, *19*, 195–208.

Chart 3. Ring-Opening Chemistry of the HNE-Derived Exocyclic 1,*N*²-dG Adducts **2** and **3** When Placed opposite dC in Duplex DNA

in this 5'-CpG-3' sequence context.⁵⁷ In the case of the crotonaldehyde adduct, the 6*R* stereoisomer formed cross-links more efficiently than did the 6*S* stereoisomer.⁵³ Of the four HNE-dG adducts (**2**–**5**), only stereoisomer **3** possessing (6*S*,8*R*,11*S*) stereochemistry resulted in DNA interchain cross-link formation.⁵¹ Significantly, this HNE isomer possessed the same relative stereochemistry as the 6*R* crotonaldehyde adduct. However, cross-link formation was slow.⁵¹ Kurtz and Lloyd⁵⁸ demonstrated that HNE adduct **3** formed a conjugate with the tetrapeptide KWKK more rapidly than did the other three stereoisomeric HNE adducts **2**, **4**, and **5**.

In the present work, we demonstrate that, similar to the related exocyclic 1,*N*²-dG adducts of acrolein⁵⁹ and crotonaldehyde,⁵⁶

when placed opposite cytosine in the dodecamer containing the 5'-C⁶pX⁷-3' sequence context (Chart 2), the diastereomeric HNE-dG adducts **2** and **3** (Chart 1) undergo ring-opening to aldehydes **6** and **10** (Chart 3); the ring-opened aldehydes exist in equilibrium with hydrated aldehydrols **7** and **11** (Chart 3). In contrast to the acrolein⁵⁹ and crotonaldehyde⁵⁶ adducts, the presence of the γ -hydroxyl group in aldehydes **6** and **10** allows for further rearrangements to cyclic hemiacetals **8** and **9**, and **12** and **13**, respectively (Chart 3), as have been observed for the Michael addition of protein nucleophiles to HNE.⁶⁰

Results

Watson–Crick Base Pairing of DNA Duplex Containing (6*R*,8*S*,11*R*) Adduct **2.** Figure 1A shows the NOE connectivity of the purine N1 and pyrimidine N3 imino protons. An imino proton resonance was observed for the modified purine X⁷. This suggested that, when placed opposite dC in this DNA duplex,

(57) Stone, M. P.; Cho, Y.-J.; Huang, H.; Kim, H.-Y.; Kozekov, I. D.; Kozekova, A.; Wang, H.; Minko, I. G.; Lloyd, R. S.; Harris, T. M.; Rizzo, C. J. *Acc. Chem. Res.* [Online early access]. DOI: 10.1021/ar700246x. Published Online: May 24, 2008. <http://pubs.acs.org/cgi-bin/abstract.cgi/achre4/asap/abs/ar700246x.html>.

(58) Kurtz, A. J.; Lloyd, R. S. *J. Biol. Chem.* **2003**, *278*, 5970–5976.

(59) de los Santos, C.; Zaliznyak, T.; Johnson, F. *J. Biol. Chem.* **2001**, *276*, 9077–9082.

(60) Sayre, L. M.; Lin, D.; Yuan, Q.; Zhu, X.; Tang, X. *Drug Metab. Rev.* **2006**, *38*, 651–675.

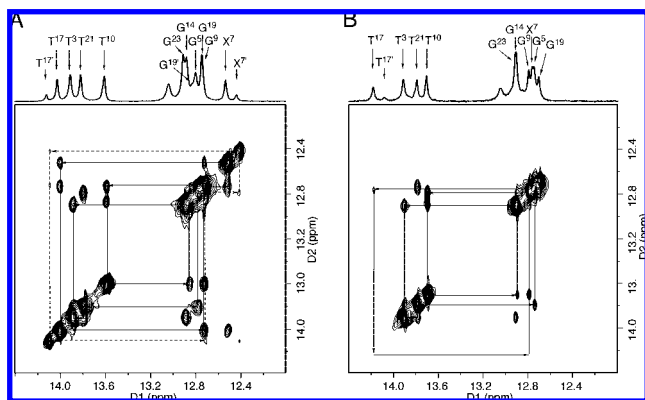


Figure 1. (A) ¹H NOESY spectra (250 ms) of the HNE-modified duplex containing stereoisomer **2** showing the sequential connectivity of the imino protons involved in hydrogen bonding. Solid lines represent the sequential connectivity pattern of the major species. Dashed lines are assigned to a minor species involving the X⁷, T¹⁷, and G¹⁹ imino protons. (B) ¹H NOESY spectra (250 ms) of the HNE-modified duplex containing stereoisomer **3** showing the sequential connectivity of the imino protons involved in hydrogen bonding. Solid lines represent the sequential connectivity pattern of the major species. The broad resonance at 14.0 ppm is assigned to the T¹⁷ imino proton of the minor species.

exocyclic 1,*N*²-dG adduct **2** had undergone ring-opening, presumably to aldehyde **6**.⁵⁹ Consequently, a complete NOE connectivity was obtained for the purine N1 and pyrimidine N3 imino protons of the duplex.⁶¹ A strong NOE was observed between X⁷ N9H → X⁷ N5H (the X⁷ amino and imino protons are designated N5H and N9H, respectively), suggesting that the exocyclic amino group X⁷ N5H was sheltered from exchange with solvent. A second NOE connectivity involving the X⁷, T¹⁷, and G¹⁹ imino protons was observed. These resonances were assigned to a minor species. Similar to the major species, the imino resonance X⁷ N9H of the minor species exhibited a cross-peak with X⁷ N5H.

Nature of the HNE-Modified Nucleotide 2. As noted, observation of imino resonances corresponding to major and minor species involving the modified purine X⁷ suggested that adduct **2** had undergone ring-opening to aldehyde **6** when placed opposite dC in this DNA duplex (Chart 3).⁵⁹ An expansion of the ¹H NMR spectrum is shown in Figure 2A. The weak resonance observed at 9.7 ppm confirmed the presence of the anticipated aldehyde. However, the aldehyde signal did not integrate proportionally with the oligodeoxynucleotide protons (Figure 2), suggesting that it was present at only trace levels and existed in equilibrium with another species.

The possibility that, upon ring-opening of adduct **2**, the resulting aldehyde **6** had further converted to aldehydrol **7** was considered (Chart 3). Aldehydes equilibrate with the corresponding aldehydrols in aqueous solution, which has been observed for the ring-opened 1,*N*²-dG adducts of acrolein and crotonaldehyde.^{55,56,59} MALDI-TOF mass spectrometric analysis yielded a molecular weight for the adducted strand of 3801.9 Da, which was inconsistent with aldehydrol **7**. The possibility that the γ -hydroxyl group could cyclize with the aldehyde in the ring-opened HNE adduct, to afford stereoisomeric cyclic hemiacetals **8** and **9**, was considered (Chart 3).^{62,63} Related

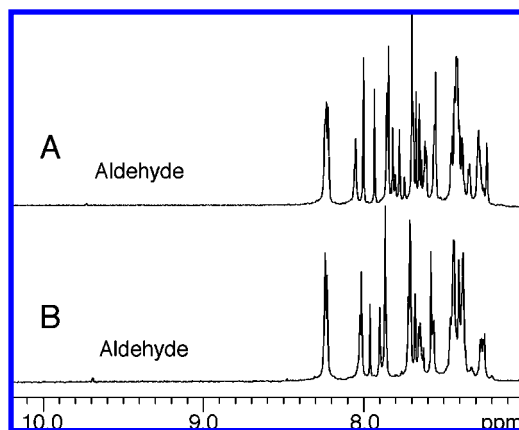


Figure 2. (A) ¹H NMR of the DNA duplex containing stereoisomer **2**, showing the aldehyde resonance at ~9.7 ppm. (B) ¹H NMR of the DNA duplex bearing stereoisomer **3**, showing the aldehyde resonance at ~9.7 ppm.

cyclic hemiacetals of cysteine, histidine, and lysine Michael addition products of HNE were characterized.⁶⁰ The calculated mass of the cyclic hemiacetal form of 3800.8 Da (M – H) was in agreement with the observed mass spectrometric analysis of 3801.8 Da. Aldehyde **6**, cyclic hemiacetals **8** and **9**, and exocyclic 1,*N*²-dG adduct **2** share the same mass. However, the NMR data (*vide infra*) were not consistent with the significant presence of exocyclic 1,*N*²-dG adduct **2** or aldehyde **6**. The existence of γ -hydroxyl group in aldehyde **6** was anticipated to facilitate formation of cyclic hemiacetals **8** and **9**. The formation of cyclic hemiacetals was not anticipated to be highly stereoselective. For example, the HNE–histidine conjugate weakly preferred the *trans* configuration of the aliphatic chain with the hydroxyl group.⁶² Thus, in agreement with the mass spectrometric data, the two sets of NMR resonances observed for the HNE protons were attributed to the formation of diastereomeric hemiacetals **8** and **9**, and not diol **7**, the latter which could exist only in a single configuration. The chemical shifts of the HNE H6 and H11 protons (Table 1) were also consistent with those observed for the cyclic hemiacetal HNE–histidine conjugates.⁶²

In the double-quantum filtered correlation spectroscopy (DQF-COSY) spectrum, a resonance observed at 5.45 ppm exhibited both dipolar and scalar couplings to a resonance observed at 2.13 ppm (Figure 3A). This was assigned as a correlation between X⁷ H8 and the vicinal X⁷ H7 ^{β} proton. Another resonance, observed at 3.93 ppm, exhibited scalar coupling to a resonance observed at 2.15 ppm (Figure 3A) and was assigned as a correlation between X⁷ H6 and the X⁷ H7 ^{α} proton. These assignments were corroborated by nuclear Overhauser effect spectroscopy (NOESY) data obtained at a mixing time of 60 ms. The difference of the chemical shifts of the two geminal X⁷ H7 protons was <0.02 ppm. Both X⁷ H7 protons exhibited NOE cross-peaks with X⁷ H6 and X⁷ H8. The correlations X⁷ H6 → X⁷ H11 and X⁷ H11 → X⁷ H12(s), observed in both NOESY and DQF-COSY spectra, were used to assign the resonances of the X⁷ H11 and X⁷ H12 protons. The resonances of X⁷ H12–H16 were overlapped. The X⁷ H6–H8, H11, and H12 resonances of the minor species were similarly assigned from DQF-COSY and NOESY spectra. Because of overlap, the X⁷ H13–H16 resonances of the minor species were not assigned. The ¹H NMR spectra of the major and the minor species were similar, although the geminal X⁷

(61) Boelens, R.; Scheek, R. M.; Dijkstra, K.; Kaptein, R. *J. Magn. Reson.* **1985**, *62*, 378–386.

(62) Hashimoto, M.; Sibata, T.; Wasada, H.; Toyokuni, S.; Uchida, K. *J. Biol. Chem.* **2003**, *278*, 5044–5051.

(63) Beretta, G.; Artali, R.; Regazzoni, L.; Panigati, M.; Facina, R. M. *Chem. Res. Toxicol.* **2007**, *20*, 1309–1314.

Table 1. ^1H Chemical Shifts of the Cyclic Hemiacetal Adducts **8** and **9** and **12** and **13**, Derived from Exocyclic $1,N^2$ -dG Adducts **2** and **3**, When Placed opposite dC in Duplex DNA

1, N^2 -dG adduct		2 (6 <i>R</i> ,8 <i>S</i> ,11 <i>R</i>)		3 (6 <i>S</i> ,8 <i>R</i> ,11 <i>S</i>)	
cyclic hemiacetal		8 (6 <i>R</i> ,8 <i>R</i> ,11 <i>R</i>) minor	9 (6 <i>R</i> ,8 <i>S</i> ,11 <i>R</i>) major	12 (6 <i>S</i> ,8 <i>S</i> ,11 <i>S</i>) minor	13 (6 <i>S</i> ,8 <i>R</i> ,11 <i>S</i>) major
chemical shift (ppm)	H6	3.85	3.93	4.15	4.55
	H7 $^{\alpha}$	1.80	2.13	1.75	2.17
	H7 $^{\beta}$	2.59	2.15	2.64	2.17
	H8	5.28	5.45	5.33	5.43
	H11	3.96	4.26	4.05	4.23
	H12 $^{\alpha}$	1.45	1.33	1.39	1.34
	H12 $^{\beta}$	1.56	1.41	1.53	1.45
	H13		1.27		1.36
	H14		1.15		1.45
	H15		1.20		1.38
	H16		0.82		0.96

H7 protons of the minor species exhibited greater chemical shift resolution. The chemical shift assignments are summarized in Table 1.

It was concluded that the major and minor species of the ring-opened HNE-dG adducts were stereoisomeric cyclic hemiacetals **8** and **9** (Chart 3). The major species showed a strong H8 \rightarrow H7 $^{\beta}$ NOE correlation and a weaker H8 \rightarrow H7 $^{\alpha}$ NOE, whereas the H6 \rightarrow H7 $^{\alpha}$ NOE was stronger than the H6 \rightarrow H7 $^{\beta}$ NOE, suggesting that X 7 H6 and X 7 H8 were in the trans

configuration. That is, cyclic stereoisomer **9** (6*R*,8*S*,11*R*) was the major species at equilibrium and stereoisomer **8** (6*R*,8*R*,11*R*) was the minor species. Modeling studies of the DNA duplex showed that the (6*R*,8*S*,11*R*) configuration agreed with the X 7 H8 \rightarrow C 18 H1', X 7 H8 \rightarrow G 19 H1', and X 7 H8 \rightarrow G 19 H4' NOEs observed for the major species.

Other Nucleotides of the Duplex Containing Stereoisomer 2. Figure 4 shows an expansion of the ^1H NOESY spectrum. The nonexchangeable protons of nucleosides were assigned on

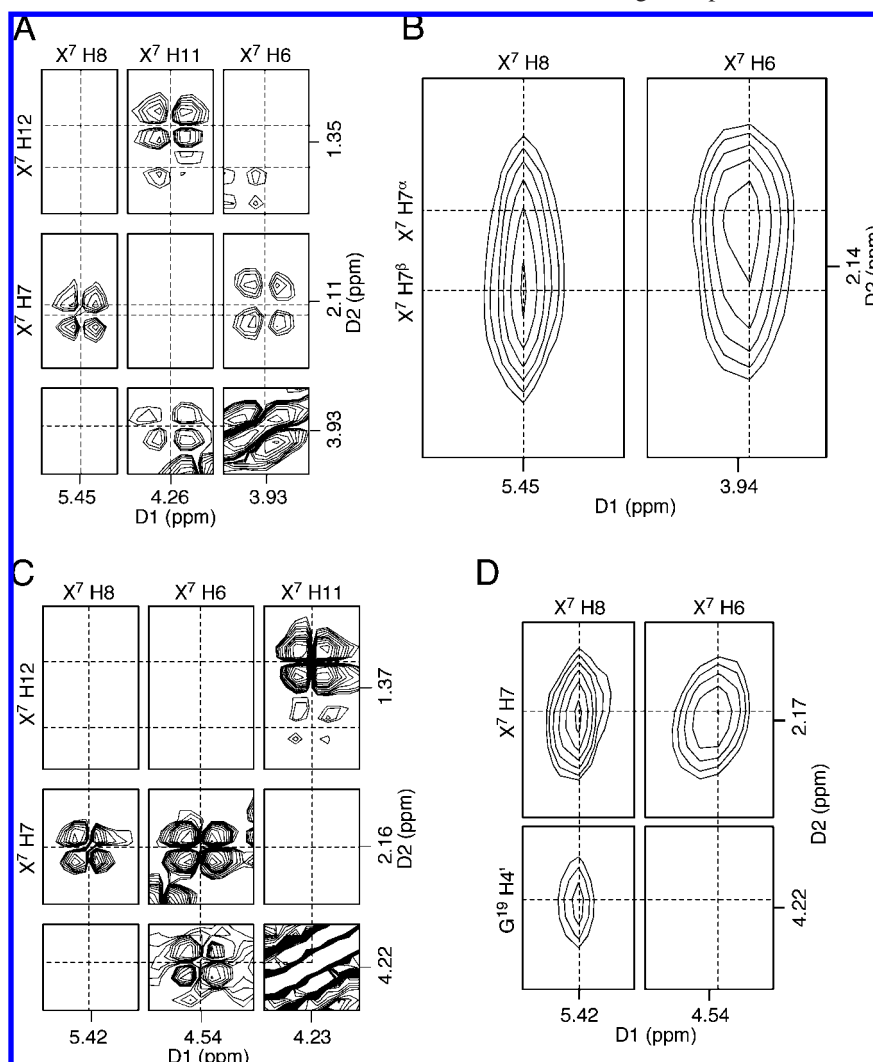


Figure 3. DQF-COSY and NOESY correlations used to assign resonances of X 7 H6–H12 protons of the major species derived from stereoisomer 2: (A) DQF-COSY and (B) NOESY (60 ms). DQF-COSY and NOESY correlations used to assign resonances of X 7 H6–H12 protons of the major species derived from stereoisomer 3: (C) DQF-COSY and (D) NOESY (60 ms).

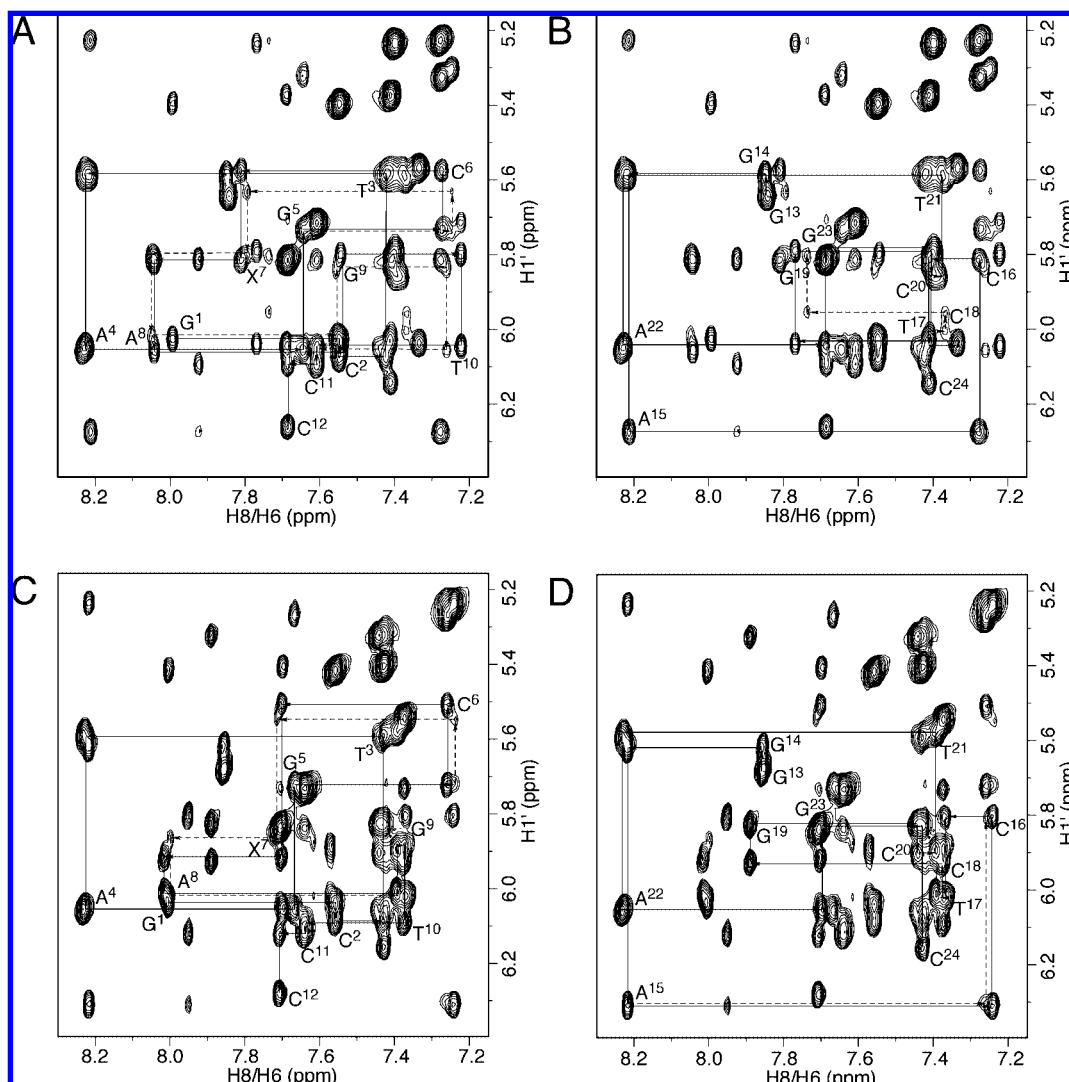


Figure 4. NOESY spectra (250 ms) of the HNE-modified duplexes containing stereoisomers **2** and **3**, showing the correlations of aromatic H6 and H8 protons with deoxyribose H1' protons. (A) Modified strand containing stereoisomer **2**. (B) Complementary strand containing stereoisomer **2**. (C) Modified strand containing stereoisomer **3**. (D) Complementary strand containing stereoisomer **3**. Solid lines indicate the major species; dotted lines represent the minor species.

the basis of the sequential connectivity of the base proton H6 or H8 (the base proton of X⁷ is designated as H2) dipolar couplings with H1' sugar protons.^{64,65} A complete sequential connectivity was observed for both the modified and the complementary strand of the major species (Figure 4A,B solid lines). A sequential connectivity was also observed for the minor species (Figure 4A,B dashed lines). In the modified strand, these extended from G⁵ → C⁶ → X⁷ → A⁸ → G⁹ → T¹⁰ → C¹¹. Most nucleoside protons of the major species as well as some protons of the minor species were assigned.

Watson–Crick Base Pairing of DNA Duplex Containing the (6*S*,8*R*,11*S*) Adduct **3.** Figure 1B shows the imino region of the NOESY spectrum. Sequential NOEs including the adducted guanine X⁷ were observed, indicating that the adduct had undergone ring-opening. The T¹⁷ N3H resonance was broad, and the diagonal peak in the NOESY spectrum was missing, suggesting that base pair A⁸·T¹⁷ was perturbed by the incorporation of stereoisomer **3**. This may contribute to the observed

4 °C lower thermal stability (*T*_m) of the DNA duplex containing stereoisomer **3** as compared to the duplex containing stereoisomer **2**.⁵¹ However, weak T¹⁷ N3H → X⁷ N9H, T¹⁷ N3H → G⁹ N1H, and T¹⁷ N3H → A⁸ H2 NOEs were observed. This suggested that the A⁸·T¹⁷ base pair adopted a weak Watson–Crick hydrogen bonding. Similar to the duplex containing stereoisomer **2**, the imino proton X⁷ N9H exhibited a strong NOE to the amino proton X⁷ N5H. A small peak was observed at 14.0 ppm and assigned as the T¹⁷ imino proton of a minor species; this signal was broad and weak when compared to the duplex of stereoisomer **2**. The anticipated imino proton resonances for X⁷ and G¹⁹ of the minor species could not be assigned because of overlapping resonances and line broadening.

Nature of the HNE-Modified Nucleotide **3.** Figure 2B shows an expansion of the ¹H NMR spectrum of the HNE-modified duplex. A weak peak was observed at ~9.7 ppm and assigned as an aldehyde. It did not integrate proportionally with the oligodeoxynucleotide protons, suggesting that the aldehyde was present in trace amounts. Mass spectrometric analysis gave a molecular mass of 3803.8 Da, in agreement with the formation of cyclic hemiacetals (calcd for M – H, 3800.8 Da), as opposed

(64) Reid, B. R. *Q. Rev. Biophys.* **1987**, *20*, 2–28.

(65) Patel, D. J.; Shapiro, L.; Hare, D. *Q. Rev. Biophys.* **1987**, *20*, 35–112.

to the aldehydrol (calcd for M - H, 3818.8 Da). As was observed for the duplex containing stereoisomer **2**, two sets of NMR resonances were observed for the HNE protons, consistent with the formation of diastereomeric hemiacetals **12** and **13** (Chart 3). The chemical shifts of the H6 and H11 HNE proton resonances were consistent with the reported chemical shifts of cyclic hemiacetal HNE-histidine conjugates.⁶²

The assignment of HNE protons followed the same strategy as that for the duplex containing stereoisomer **2** (Table 1). Of note, the geminal H7 protons of the major species were not resolved (Figure 3C,D) for **3**. NOESY spectra revealed that X⁷ H8 strongly correlated with G¹⁹ H4'. A strong NOE cross-peak was observed at 60-ms mixing time (Figure 3D), indicating that X⁷ H8 and G¹⁹ H4' were proximate. Modeling studies indicated that the R configuration of X⁷ C8 placed X⁷ H8 2.4–3.6 Å from G¹⁹ H4'. In contrast, the S configuration of X⁷ C8 placed X⁷ H8 4.0–5.1 Å from G¹⁹ H4'. Therefore, the strong X⁷ H8 → G¹⁹ H4' NOE suggested that cyclic hemiacetal stereoisomer **13** (6*S*,8*R*,11*S*) was the major species derived from the ring-opening of HNE adduct **3**, and consequently, stereoisomer **12** (6*S*,8*S*,11*S*) was the minor species (Chart 3). Modeling studies of the DNA duplex also showed that the (6*S*,8*R*,11*S*) configuration agreed well with X⁷ H8 → C¹⁸ H1', X⁷ H8 → G¹⁹ H1', X⁷ H8 → G¹⁹ H5', and X⁷ H8 → G¹⁹ H5'' correlations. Some HNE resonances of the minor species were assigned on the basis of DQF-COSY and NOESY spectra. In contrast to the major species, the geminal X⁷ H7 protons of the minor species were resolved. Because of overlap, the X⁷ H13–H16 resonances of the minor species were not assigned (Table 1). Except for X⁷ H6, all HNE protons of the major species derived from stereoisomers **2** and **3** had similar chemical shifts, indicating similar structures. The X⁷ H6 protons derived from stereoisomers **2** and **3** exhibited a chemical shift difference of 0.62 ppm, indicating different chemical environments of the X⁷ H6 protons for these stereoisomers.

Other Nucleotides of the Duplex Containing Stereoisomer 3. Figure 4C,D shows an expansion of the ¹H NOESY spectrum. The nonexchangeable protons of the nucleotides were assigned on the basis of the sequential connectivity of the base proton H6 or H8 (the base proton of X⁷ is designated as H2) dipolar couplings with H1' sugar protons.^{64,65} A complete sequential connectivity was observed for both the modified and the complementary strand (Figure 4C,D solid lines). A second sequential connectivity was observed (Figure 4C,D dashed lines). In the modified strand, these extended from C⁶ → X⁷ → A⁸. These were assigned to the minor species.

Discussion

The Michael addition of HNE to deoxyguanosine in DNA gives four diastereomeric exocyclic 1,*N*²-deoxyguanosine adducts (**2–5**) (Chart 1).^{27–29,57} Incorporation of the exocyclic 1,*N*²-dG structure into duplex DNA precludes Watson–Crick hydrogen bonding and results in structural^{66–69} and thermodynamic⁷⁰ perturbations at the lesion and complementary nucle-

otides. On the basis of observations with the corresponding exocyclic 1,*N*²-dG adducts arising from acrolein⁵⁹ and crotonaldehyde⁵⁶ in DNA, it was anticipated that the adducts **2–5** (Chart 1) would undergo ring-opening to aldehydes when placed opposite cytosine in duplex DNA. The resulting aldehydes might then form interstrand cross-links in the 5'-CpG-3' sequence.^{52–57} Significantly, when HNE adducts **2–5** were incorporated into the dodecamer containing the 5'-CpX-3' sequence (Chart 2) and examined as to their respective abilities to form interstrand cross-links, only stereoisomer **3** formed interstrand cross-links.⁵¹ Consequently, it was of interest to examine in greater detail the structure of the non-cross-linking stereoisomer **2** vs that of the cross-linking stereoisomer **3** when placed into duplex DNA opposite cytosine. The specific comparison of stereoisomers **2** vs **3** was also relevant because they possessed the same relative stereochemistry at C6 as did the corresponding 6*R* and 6*S* stereoisomers of the crotonaldehyde adduct, of which the 6*R* adduct formed interstrand cross-links much more efficiently⁵³ (note that the R vs S designation at C6 is reversed for the HNE adducts as compared to that of the crotonaldehyde adducts).⁵¹ Moreover, both HNE stereoisomers induced low levels of G → T mutations in the mammalian COS-7 cell assay, whereas stereoisomers **4** and **5** were largely inactive in the site-specific mutagenesis studies.⁴⁷

HNE-Derived Exocyclic 1,*N*²-dG Adducts 2 and 3 Rearrange to Diastereomeric *N*²-dG Cyclic Hemiacetal Adducts When Placed opposite Cytosine in Duplex DNA. The HNE-derived 1,*N*²-dG adducts **2** and **3** bear exocyclic rings through the bonding of guanine N1 and *N*² to the HNE moiety; Watson–Crick hydrogen bonding is not possible. The NMR data indicate that when either exocyclic adduct **2** or **3** was placed into duplex DNA opposite cytosine, ring-opening to aldehydes **6** and **10** occurred (Chart 3, Figures 1 and 2). Riggins et al.^{71,72} reported mechanistic studies of the ring-opening and -closing of the structurally related malondialdehyde-derived adduct 3-(2'-deoxy-β-D-erythroptofuranosyl)pyrimido[1,2-α]purin-10(3*H*)-one (M₁dG). They concluded that ring-opening of M₁dG as a nucleoside or in oligodeoxynucleotides occurred via a reversible second-order reaction with hydroxide ion and was catalyzed by the complementary cytosine in duplex DNA. The closure of the resulting *N*²-(3-oxo-1-propenyl)deoxyguanosine anion was pH-dependent, and under neutral and acidic conditions ring closure was biphasic, leading to the rapid formation of intermediates that slowly converted to M₁dG in a general-acid-catalyzed reaction.

In contrast to the corresponding acrolein⁵⁹ and crotonaldehyde⁵⁶ adducts, the major forms of the ring-opened species arising from HNE adducts **2** or **3** were not the aldehydes **6** and **10** when at equilibrium in duplex DNA (Chart 3). Only trace amounts of aldehydes **6** and **10** were derived from the ring-opening of exocyclic 1,*N*²-dG adducts **2** and **3**. For the exocyclic 1,*N*²-dG adducts derived from acrolein⁵⁹ and crotonaldehyde⁵⁶ in an identical sequence, the ring-opened aldehydes were observed to be in equilibrium with the corresponding aldehydrols. However, our spectroscopic data indicate that cyclic hemiacetals **8** and **9**, or **12** and **13**, arise from HNE adducts **2** or **3**, respectively (Chart 3). Starting from adduct **2**, cyclic hemiacetal stereoisomer **9** (6*R*,8*S*,11*R*) is the major species at equilibrium, and stereoisomer **8** (6*R*,8*R*,11*R*) is the minor

(66) Kouchakdjian, M.; Marinelli, E.; Gao, X.; Johnson, F.; Grollman, A.; Patel, D. *Biochemistry* **1989**, *28*, 5647–5657.

(67) Kouchakdjian, M.; Eisenberg, M.; Live, D.; Marinelli, E.; Grollman, A. P.; Patel, D. J. *Biochemistry* **1990**, *29*, 4456–4465.

(68) Singh, U. S.; Moe, J. G.; Reddy, G. R.; Weisenseel, J. P.; Marnett, L. J.; Stone, M. P. *Chem. Res. Toxicol.* **1993**, *6*, 825–836.

(69) Weisenseel, J. P.; Reddy, G. R.; Marnett, L. J.; Stone, M. P. *Chem. Res. Toxicol.* **2002**, *15*, 127–139.

(70) Plum, G. E.; Grollman, A. P.; Johnson, F.; Breslauer, K. J. *Biochemistry* **1992**, *31*, 12096–12102.

(71) Riggins, J. N.; Pratt, D. A.; Voehler, M.; Daniels, J. S.; Marnett, L. J. *J. Am. Chem. Soc.* **2004**, *126*, 10571–10581.

(72) Riggins, J. N.; Daniels, J. S.; Rouzer, C. A.; Marnett, L. J. *J. Am. Chem. Soc.* **2004**, *126*, 8237–8243.

species. Likewise, starting from adduct **3**, cyclic hemiacetal stereoisomer **13** (6*S*,8*R*,11*S*) is the major species, and stereoisomer **12** (6*S*,8*S*,11*S*) is the minor species. The stereochemistry of the cyclic hemiacetal presumably avoids steric repulsion from the large substituent groups. Detailed structural refinement of these DNA duplexes (Chart 2) containing either stereoisomers **9** or **13** is in progress.

Chemical and Biological Implications. The formation of interchain DNA cross-link of enal adducts of dG is intrinsically slow, on the order of days for the acrolein adduct and weeks for the crotonaldehyde adduct.^{52,53} The formation of cyclic hemiacetals **12** and **13** (Chart 3) may, in part, explain the slower rate of interstrand cross-link formation by HNE adduct **3** in the 5'-CpG-3' sequence.⁵¹ The cyclic hemiacetals **12** and **13** mask the reactive aldehyde **10** necessary for formation of the interstrand 5'-CpG-3' cross-link. Notably, HNE adduct **2** does not form interstrand cross-links in the 5'-CpG-3' sequence,⁵¹ despite the fact that it also undergoes ring-opening when placed opposite dC in duplex DNA, to form trace amounts of aldehyde **6**. We surmise that the explanation probably involves stereospecific differences in the conformation of aldehyde **6** as compared to that of aldehyde **10**, within the minor groove of duplex DNA. The detailed structural refinement of these DNA duplexes (Chart 2) containing either stereoisomers **9** or **13**, in progress, will be of considerable interest. The slow rate of formation of DNA-peptide conjugates by either HNE adduct **2** or **3**⁵⁸ may also be attributed to the preference for formation of cyclic hemiacetals **8** and **9**, or **12** and **13**, respectively. In fact, the four exocyclic 1,N²-dG stereoisomers **2**–**5** arising from HNE formed DNA-peptide conjugates,⁵⁸ consistent with the observation that HNE adducts **2** and **3** undergo ring-opening to trace amounts of aldehydes **6** and **10**, and inferring that adducts **4** and **5** (Chart 1) share similar chemistry in duplex DNA.

It has been suggested that the low levels of G → T mutations observed when site-specific mutagenesis of adducts **2** and **3** was examined in mammalian cells may be attributable to the rearrangement of these adducts into the cyclic hemiacetals **8** and **9**, and **12** and **13**, respectively, because this rearrangement may facilitate formation of Watson-Crick hydrogen bonding during replication bypass of the lesions.⁴⁷ Xing et al.⁷³ attributed high levels of G → T mutations to the ring-closed 1,N²-dG adducts. Similar explanations have been advanced to explain the low levels of mutations induced by the acrolein^{74,75} and crotonaldehyde-derived exocyclic 1,N²-dG adducts,⁷⁶ as compared to the 1,N²-propano-dG (PdG) adduct which remains in the exocyclic form.^{77,78} Stein et al.⁷⁹ reported higher levels of mutations for the crotonaldehyde adducts, which may be attributable to a greater amount of the exocyclic 1,N²-dG adducts in duplex DNA.⁵⁶ The low levels of the exocyclic 1,N²-dG adducts, observed spectroscopically when either adducts **2** or **3** are placed opposite dC in duplex DNA, are consistent with this

hypothesis. With regard to lesion bypass, DNA polymerase η cannot bypass the HNE-derived exocyclic 1,N²-dG adducts.⁸⁰ This contrasted with its ability to bypass the less bulky acrolein-derived exocyclic 1,N²-dG adduct,⁸⁰ suggesting that the larger HNE adducts disrupt the active site of this Y-family polymerase. However, the sequential action of human pols ι and κ was able to carry out error-free bypass and extension of the (6*S*,8*R*,11*R*) and (6*S*,8*R*,11*S*) diastereomers of the HNE adduct.⁸¹ In this case, pol ι inserted dCTP, perhaps involving Hoogsteen pairing, and to a lesser extent dTTP opposite the HNE adduct but was unable to further elongate the primer. Further extension was observed in the presence of pol κ , which elongated from a C opposite the HNE adducts much more efficiently than when T was opposite the adducts.⁸¹ Therefore, further conformational analyses of these HNE-derived exocyclic 1,N²-dG adducts in both duplex DNA and in complexes with Y-family polymerases will be of interest.

Conclusions

The chemistry of the HNE-derived exocyclic 1,N²-dG adduct **3** of (6*S*,8*R*,11*S*) stereochemistry was compared with that of the corresponding (6*R*,8*S*,11*R*) adduct **2**, when incorporated into duplex DNA. At pH 7, both stereoisomeric adducts **2** and **3** underwent ring-opening to aldehydic rearrangement products **6** and **10**, respectively, suggesting that the slow interstrand cross-link formation in DNA containing 5'-CpG-3' sequence context by the exocyclic 1,N²-dG adduct **3** of (6*S*,8*R*,11*S*) stereochemistry, and the lack of interstrand cross-link formation by the exocyclic 1,N²-dG adduct **2** of (6*R*,8*S*,11*R*) stereochemistry, was not attributable to their inability to undergo ring-opening to reactive aldehydes **6** and **10**. Instead, these aldehydes existed in equilibrium with stereoisomeric cyclic hemiacetals **8** and **9**, and **12** and **13**. Cyclic hemiacetals **9**, arising from adduct **2**, and **13**, arising from adduct **3**, were the predominant species present at equilibrium. Cyclic hemiacetals **12** and **13** mask the reactive aldehydes **6** and **10** necessary for interstrand cross-link formation, and their presence may, in part, explain the slow interstrand cross-link formation in DNA containing 5'-CpG-3' sequence context by the exocyclic 1,N²-dG adduct **3** of (6*S*,8*R*,11*S*) stereochemistry.

Experimental Methods

Materials. The oligodeoxynucleotide 5'-d(GGACTCGCTAGC)-3' was synthesized and purified by anion-exchange chromatography by the Midland Certified Reagent Co. The oligonucleotides containing HNE-derived exocyclic 1,N²-dG adducts **2** and **3** in the dodecamer 5'-d(GCTAGCXAGTCC)-3', where X represents the HNE-dG adducts, were synthesized, purified, and characterized as reported.^{50,51} The purities of the adducted oligodeoxynucleotides were assessed by capillary gel electrophoresis and HPLC. Oligodeoxynucleotides were desalted by chromatography on Sephadex G-25.

Mass Spectrometry of the HNE Adducts in Duplex Oligodeoxynucleotides. The duplex oligodeoxynucleotides containing either stereoisomeric HNE adducts **2** or **3** were analyzed by mass spectrometry. The concentrations of the oligonucleotides were determined by UV absorption at 260 nm, and the extinction coefficients of both sequences were calculated as $1.12 \times 10^5 \text{ L mol}^{-1} \text{ cm}^{-1}$.⁸² The strands were annealed in buffer containing 10

(73) Xing, D. X.; Sun, L. X.; Cukier, R. I.; Bu, Y. X. *J. Phys. Chem. B* **2007**, *111*, 5362–5371.

(74) VanderVeen, L. A.; Hashim, M. F.; Nechev, L. V.; Harris, T. M.; Harris, C. M.; Marnett, L. J. *J. Biol. Chem.* **2001**, *276*, 9066–9070.

(75) Yang, I. Y.; Hossain, M.; Miller, H.; Khullar, S.; Johnson, F.; Grollman, A.; Moriya, M. *J. Biol. Chem.* **2001**, *276*, 9071–9076.

(76) Fernandes, P. H.; Kanuri, M.; Nechev, L. V.; Harris, T. M.; Lloyd, R. S. *Environ. Mol. Mutagen.* **2005**, *45*, 455–459.

(77) Moriya, M.; Zhang, W.; Johnson, F.; Grollman, A. P. *Proc. Natl. Acad. Sci. U.S.A.* **1994**, *91*, 11899–11903.

(78) Moriya, M.; Pandya, G. A.; Johnson, F.; Grollman, A. P. *IARC Sci. Publ.* **1999**, *150*, 263–270.

(79) Stein, S.; Lao, Y.; Yang, I. Y.; Hecht, S. S.; Moriya, M. *Mutat. Res.* **2006**, *608*, 1–7.

(80) Minko, I. G.; Washington, M. T.; Kanuri, M.; Prakash, L.; Prakash, S.; Lloyd, R. S. *J. Biol. Chem.* **2003**, *278*, 784–790.

(81) Wolfe, W. T.; Johnson, R. E.; Minko, I. G.; Lloyd, R. S.; Prakash, S.; Prakash, L. *Mol. Cell. Biol.* **2006**, *26*, 381–386.

(82) Cavaluzzi, M. J.; Borer, P. N. *Nucleic Acids Res.* **2004**, *32*, e13.

mM NaH₂PO₄, 100 mM NaCl, and 50 μM Na₂EDTA (pH 7.0). The solution containing the modified and complementary oligodeoxynucleotides at 1:1 stoichiometry was heated to 95 °C for 10 min, then slowly cooled to room temperature. The duplex DNA was purified by DNA-grade hydroxylapatite chromatography with a gradient from 10 to 200 mM NaH₂PO₄ in 100 mM NaCl, 50 μM Na₂EDTA (pH 7.0), and then desalted by Sephadex G-25. The duplexes were identified by MALDI-TOF mass spectroscopy on Voyager-DE STR spectrometer (Applied Biosystems, Inc.). The oligodeoxynucleotide duplex was dissolved in distilled water or 50 mM NaCl to form a 0.5 mM strand concentration solution. One microliter of the oligodeoxynucleotide duplex solution was combined with 1 μL of hydroxypicolinic acid matrix solution and dried at room temperature.

The MALDI-TOF mass spectrum of the duplex oligodeoxynucleotide containing stereoisomer **2** showed a mass for the modified strand of *m/z* 3801.9 (calcd for M - H, 3800.9), and a mass of *m/z* of 3645.4 for the complementary strand (calcd for M - H, 3645.4). A mass of *m/z* of 3824.8 was observed for the modified strand (calcd for M + Na - 1, 3823.9) in 50 mM NaCl solution. The complementary strand was observed at *m/z* of 3647.0. The MALDI-TOF mass spectrum of the duplex oligodeoxynucleotide containing stereoisomer **3** showed a mass for the modified strand of *m/z* 3803.8 (calcd for M - H, 3800.9), a mass of *m/z* 3645.2 for the complementary strand (calcd for M - H, 3645.4). A mass corresponding to the duplex containing **3** at *m/z* 7451.0 (calcd for M - H, 7447.3) was also observed. A mass of *m/z* 3802.7 was observed for the modified strand in 50 mM NaCl solution. The complementary strand was observed at *m/z* 3646.4.

NMR. Samples were at 1.0 mM strand concentration. Samples for the nonexchangeable protons were dissolved in 280 μL of a buffer containing 10 mM NaH₂PO₄, 100 mM NaCl, 50 μM Na₂EDTA (pH 7.0). They were exchanged with D₂O and suspended in 280 μL of 99.996% D₂O. The pH was adjusted to 7.0 with dilute DCl or NaOD solutions. Samples for the observation of exchangeable protons were dissolved in 280 μL of 10 mM NaH₂PO₄, 100 mM NaCl, 50 μM EDTA (pH 7.0) containing 9:1 H₂O/D₂O (v/v),

and the pH was adjusted to 7.0. NMR experiments were performed on a Bruker Avance 800 spectrometer with a cryogenic probe (Bruker Instruments). The temperature was 25 °C for observation of the nonexchangeable protons and 5 °C for observation of the exchangeable protons. Chemical shifts for ¹H were referenced to water. Data were processed using FELIX 2000 (Accelrys, Inc.) on Silicon Graphics workstations (Silicon Graphics, Inc.). For all NMR experiments, a relaxation delay of 1.5 s was used. Two-dimensional homonuclear NMR spectra were recorded with 512 real data in the t₂ dimension and 2048 real data in the t₁ dimension. NOESY spectra were zero-filled during processing to create a matrix of 1024 × 1024 real points, and other spectra were zero-filled to create a matrix of 1024 × 512 real points. A skewed sinebell-square apodization with 15° phase shift was used in both dimensions to process COSY spectra. The total correlation spectroscopy mixing time was 80 ms for the duplex containing stereoisomer **2** and 100 ms for the duplex containing stereoisomer **3**. For assignment of exchangeable protons, NOESY experiments used the watergate sequence.⁸³ The mixing time was 250 ms. For assignment of nonexchangeable protons and the derivation of distance restraints, NOESY experiments used TPPI quadrature detection and mixing times of 60 and 250 ms were used. DQF-COSY experiments were performed with TPPI quadrature detection and presaturation of the residual water during the relaxation delay.

Acknowledgment. Dr. Markus Voehler assisted with NMR experiments. Drs. Constance M. Harris and Thomas M. Harris provided thoughtful comments regarding the chemistry of these adducts. This work was supported by NIH Grant ES-05355 (C.J.R. and M.P.S.). The Vanderbilt University Center in Molecular Toxicology is supported by NIH Grant P30 ES-00267.

JA801824B

(83) Piotto, M.; Saudek, V.; Sklenar, V. *J. Biomol. NMR* **1992**, *2*, 661-665.